PNAS RESEARCH ARTICLE | DEVELOPMENTAL BIOLOGY

Noncanonical function of Capicua as a growth termination signal in *Drosophila* oogenesis

Laura Rodríguez-Muñoz[a], Clàudia Lagares[a], Sergio González-Crespo[a], Pau Castel[b], Alexey Veraksa[c], and Gerardo Jiménez[a,d,1]

Edited by Norbert Perrimon, Harvard Medical School, Boston, MA; received December 29, 2021; accepted June 10, 2022

Capicua (Cic) proteins are conserved HMG-box transcriptional repressors that control receptor tyrosine kinase (RTK) signaling responses and are implicated in human neurological syndromes and cancer. While Cic is known to exist as short (Cic-S) and long (Cic-L) isoforms with identical HMG-box and associated core regions but distinct N termini, most previous studies have focused on Cic-S, leaving the function of Cic-L unexplored. Here we show that Cic-L acts in two capacities during *Drosophila* oogenesis: 1) as a canonical sensor of RTK signaling in somatic follicle cells, and 2) as a regulator of postmitotic growth in germline nurse cells. In these latter cells, Cic-L behaves as a temporal signal that terminates endoreplicative growth before they dump their contents into the oocyte. We show that Cic-L is necessary and sufficient for nurse cell endoreplication arrest and induces both stabilization of CycE and down-regulation of Myc. Surprisingly, this function depends mainly on the Cic-L–specific N-terminal module, which is capable of acting independently of the Cic HMG-box–containing core. Mirroring these observations, basal metazoans possess truncated Cic-like proteins composed only of Cic-L N-terminal sequences, suggesting that this module plays unique, ancient roles unrelated to the canonical function of Cic.

Capicua | RTK signaling | endoreplicative growth | oogenesis | *Drosophila*

Significance

Capicua (Cic) is a conserved HMG-box transcriptional repressor and tumor suppressor regulated by receptor tyrosine kinase signaling. Here, we report that a highly conserved yet uncharacterized Cic isoform called Cic-L has both canonical and noncanonical functions in *Drosophila* oogenesis. The noncanonical function takes place in oocyte-associated germline cells, which grow through polyploidization until Cic-L halts their growth and allows them to empty their contents into the oocyte. Unexpectedly, this function does not critically depend on the characteristic HMG-box domain and is instead mediated by the unique Cic-L N-terminal module. In fact, this module appears to have originated before Cic proteins acquired an HMG-box, suggesting that it plays ancient, autonomous functions that may be conserved across metazoans.

The HMG-box protein Capicua (Cic) has emerged as an important developmental regulator with key roles in human neurological syndromes and cancer (1–11) (reviewed in refs. 12, 13). Cic functions antagonistically to the receptor tyrosine kinase (RTK)-Ras-MAPK signaling pathway: it represses RTK-induced genes in the absence of signaling and is in turn phosphorylated and inhibited upon RTK activation, which thus releases repression of Cic targets (4, 14–16). Studies in *Drosophila* and mammalian systems have revealed the salient features of Cic activity and regulation, including its ability to bind specific DNA sequences through the HMG-box and a C-terminal auxiliary domain called C1 (17, 18), and respond to RTK control via MAPK docking sites (14, 19). Notably, these studies have also shown that in all these species, Cic exists as short (Cic-S) and long (Cic-L) isoforms with different N-terminal regions (12, 20). However, the function(s) of Cic-L and its conserved N terminus has remained virtually unknown. Here we show that the Cic-L N terminus is an ancient protein module with unique functional properties unrelated to the canonical RTK–Cic switch.

To study Cic-L, we have focused on *Drosophila* oogenesis as a model system. Oogenesis is the process that provides the oocyte with maternal factors and organelles that are essential for totipotency and successful development into the next generation. In species ranging from *Hydra* to mammals, oocytes develop in association with auxiliary cells that both supply the oocyte with such materials and control its development and maturation (21–24). In *Drosophila*, two types of oocyte-associated cells are present: nurse cells (NCs) and follicle cells (FCs). There are 15 germline NCs born together with the oocyte after four mitotic divisions of a primary cystoblast. Due to incomplete cytokinesis during these divisions, the 16 cells remain connected forming a cyst, which permits the transfer of cytoplasmic components from the NCs to the oocyte. The NCs are highly biosynthetically productive due to a program of DNA endoreplication cycles (endocycles), in which NCs successively replicate their genome without division, thus becoming large polyploid cells (25–27). The NCs then feed the oocyte in two differentiated phases: an early, slow phase of cytoplasmic transfer concurrent with NC growth (stages 2 through 10A), and a late phase in which the NCs rapidly "dump" all their cytoplasmic contents into the oocyte and die (stages 10B through 14) (21, 28–30). On the other hand, the somatic FCs form an epithelium that surrounds each NC-oocyte cyst. The FCs exchange intercellular signals with the oocyte to regulate the body axes of the future embryo (31, 32), secrete eggshell layers that protect the mature egg, and contribute to eliminate residual NC corpses once dumping is completed (28).

Author affiliations: [a]Department of Developmental Biology, Instituto de Biología Molecular de Barcelona, Consejo Superior de Investigaciones Científicas, Barcelona, 08028 Spain; [b]Department of Biochemistry and Molecular Pharmacology, New York University Grossman School of Medicine, New York, NY 10016; [c]Department of Biology, University of Massachusetts, Boston, MA 02125; and [d]Institució Catalana de Recerca i Estudis Avançats, 08010 Barcelona, Spain

Author contributions: L.R.-M., C.L., and G.J. designed research; L.R.-M. and C.L. performed research; L.R.-M., C.L., S.G.-C., P.C., A.V., and G.J. analyzed data; and L.R.-M., C.L., and G.J. wrote the paper.

The authors declare no competing interest.

This article is a PNAS Direct Submission.

[1]To whom correspondence may be addressed. Email: gjcbmc@ibmb.csic.es.

This article contains supporting information online at http://www.pnas.org/lookup/suppl/doi:10.1073/pnas.2123467119/-/DCSupplemental.

Published July 26, 2022.

Here we demonstrate that Cic-L functions redundantly with Cic-S in FCs during the establishment of embryonic dorsoventral (DV) polarity, a process regulated by canonical RTK–Cic interactions (14, 33, 34). In addition, Cic-L acts individually in NCs by inducing NC endocycle exit and enabling cytoplasmic dumping into the oocyte. This exclusive function is mediated, at least in part, through stabilization of cyclin E (CycE) and down-regulation of Myc, two key regulators of endoreplicative growth (35–38). Surprisingly, Cic-L–specific activity does not critically depend on its DNA-binding HMG-box and C1 domains but instead is exerted by its unique N-terminal region. Mirroring these structural requirements, we also note that truncated Cic-like proteins composed only of Cic-L N-terminal sequences are present in basal metazoan phyla, namely sponges and placozoans. Our findings thus expand the functional scope of Cic family proteins beyond their canonical roles as DNA-binding transcriptional repressors connected to RTK signaling.

Results

The Cic-L N Terminus Is an Ancient Protein Module. Cic family proteins are highly conserved from cnidarians to humans, sharing a characteristic core region that includes the HMG-box and C1 DNA-binding domains (12, 18). Cic-L proteins contain, in addition, a unique ~750- to 850-residue N-terminal extension with at least two conserved domains, N1 (12, 20), and a Tudor-like domain (39). While exploring the conservation of these domains, we noted that they are present in two basal metazoans, the sponge *Amphimedon* and the placozoan *Trichoplax*, but without an associated Cic core, which seems to be missing altogether in those organisms (Fig. 1 *A* and *B* and *SI Appendix*, Fig. S1). This was unexpected because this core is essential for all known Cic functions in any system. Nevertheless, several lines of evidence support the validity of these genome-based predictions. First, we verified the structure of the *Amphimedon* N1-encoding gene (*LOC100637684*) using deep RNA-sequencing (RNA-seq) data from this species (40). Second, the structure of the *Trichoplax* ortholog gene (designated *TRIADDRAFT_56001* or *TrispH2_004367*) has been confirmed after sequencing the genomes of two independent *Trichoplax* lineages (41, 42). Third, conceptual translation of a 120-kb genomic fragment spanning the *TRIADDRAFT_56001* locus and several adjacent predicted genes did not reveal sequences potentially encoding an HMG-box or a C1-like domain. Together, these observations suggest that these Cic-L–like proteins may represent extant orthologs of a putative Cic ancestor that lacked the HMG-box and C1 domains, and we therefore refer to them as "Proto-Cic" (Fig. 1*A*). Furthermore, these Proto-Cic forms pointed to an intrinsic activity of Cic-L N-terminal domains that could confer unique functional properties to the full-length protein. Consistent with these ideas, vertebrate Cic-L predicted structures identify N1 and Tudor-like as well-folded, potentially functional domains (Fig. 1*C* and *SI Appendix*, *Supplementary Materials and Methods*).

Cic-L and Cic-S Act Redundantly in Ovarian Follicle Cells. To explore these potential unique properties, we have used *Drosophila* as a model system. Because Cic-L had not been visualized individually in *Drosophila*, we began by characterizing its expression relative to that of Cic-S (see *Materials and Methods* for a description of the isoforms studied here). To this end, we generated a *cic-L*^{HA} knockin line, which carries tandem HA epitopes inserted into the unique *cic-L* coding region and is phenotypically normal (Fig. 2*A*). We then combined this line with a transgenic rescue construct expressing Cic-S tagged with Venus (Fig. 2*A*) (1, 43) and compared the distributions of both isoforms in different tissues. In particular, we found that both isoforms are coexpressed throughout oogenesis (Fig. 2 *B* and *B*′), although with significant differences as described below.

First, Cic-L and Cic-S are both detectable in FCs from stage 2 onwards. This caught our attention because Cic functions in FCs during midoogenesis to regulate embryonic DV polarity downstream of EGFR/RTK signaling (14, 33, 34). Specifically, Cic represses Mirror (Mirr) transcription factor expression in ventral FCs, but not in dorsal FCs where Cic is down-regulated by EGFR signaling (14, 33, 34, 44) (Fig. 2*B*′ and *SI Appendix*, Fig. S2*A*). We therefore reasoned that this setting would offer the opportunity to analyze the relationship between Cic-L and Cic-S.

To study Cic-L function in this context, we generated a CRISPR-induced mutation, *cic*^{7}, which bears a frameshift lesion within the N1 domain and is a presumed null allele of *cic-L* (Fig. 2*A*). In homozygosis, *cic*^{7} causes lethality during larval and pupal stages, indicating that Cic-L is essential in *Drosophila*. We then used *cic*^{7} and a *cic-S*–specific allele, *cic*^{5} (Fig. 2*A*), to examine the effects of each mutation on DV patterning. In this system, loss of Cic function derepresses Mirr expression and causes dorsalization of the future embryo (18, 33, 44, 45) (*SI Appendix*, Fig. S2*A*). When assaying each mutation in trans to *cic*^{4}, a strong hypomorph that maps to the Cic core and impairs all known Cic functions (Fig. 2*A*, see also below), we did not observe dorsalization defects, as monitored

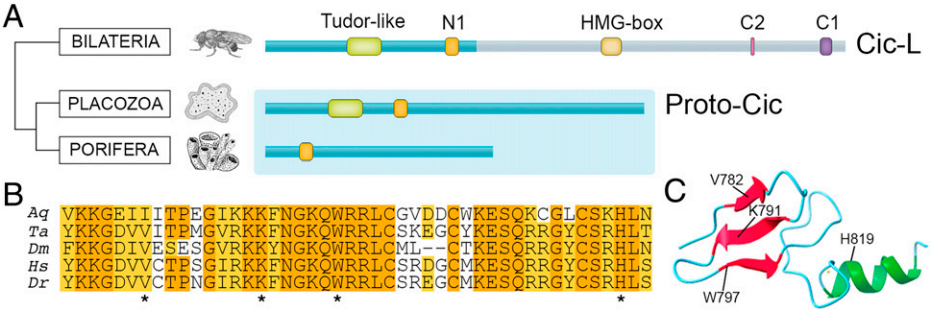

Fig. 1. Structure and evolutionary conservation of the Cic-L N terminus. (*A*) Domain structure and phylogenetic relationships of Cic-L–related proteins from *Drosophila*, *Trichoplax*, and *Amphimedon*. The N1 and Tudor-like domains are indicated. (*B*) Alignment of N1 amino acid sequences from *Amphimedon queenslandica* (*Aq*), *Trichoplax adhaerens* (*Ta*), *Drosophila melanogaster* (*Dm*), human (*Hs*), and zebrafish (*Danio rerio*, *Dr*). Identical and similar residues are indicated by dark and light shading, respectively. Note the abundance of basic residues and the presence of three closely spaced cysteine residues. Asterisks mark selected residues that are highlighted in *C*. (*C*) Structure of N1 domain from zebrafish Cic-L as predicted by AlphaFold (76). The ribbon representation shows three β-strands (red) and a single α-helix (green).

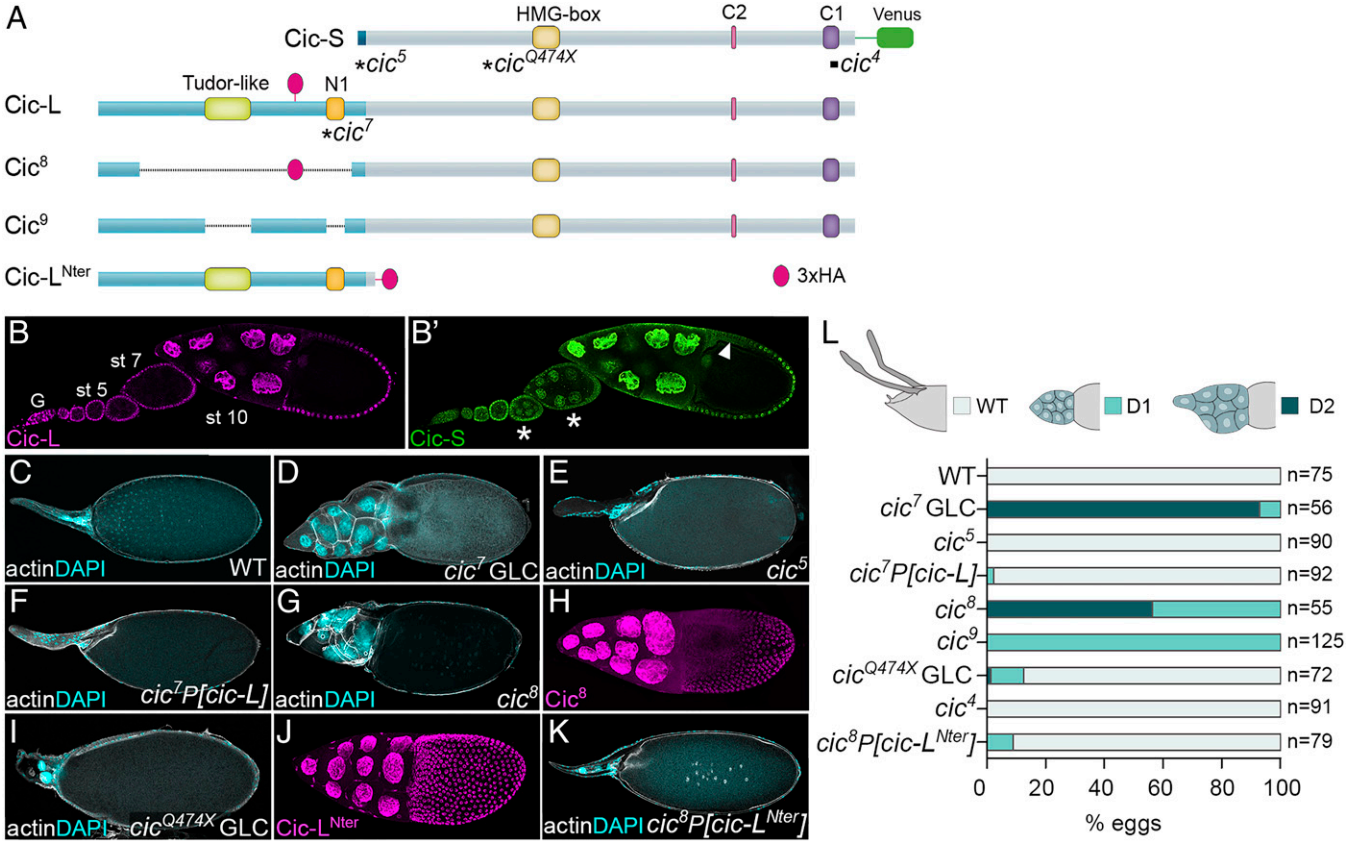

Fig. 2. Cic-L activity in NCs relies on its distinctive N-terminal domain. (*A*) Modular structure of Cic isoforms and Cic-L mutant derivatives showing their common and unique domains and the position of selected *cic* mutations. Frameshift mutations are marked with asterisks and the cic^4 deletion is indicated by a thick line. The Venus and HA tags used in this study are also indicated. (*B*) Ovariole expressing Cic-L^{HA} and Cic-S^{Venus} and stained with anti-HA (*B*) and anti-GFP (*B′*) antibodies. Asterisks in *B′* mark expression of Cic-S^{Venus}, but not Cic-L^{HA}, in stage-5 to stage-7 NCs. G, germarium. Arrowhead in *B′* points to cytoplasmic relocalization of Cic-S, but not Cic-L, in dorsal–anterior FCs exposed to EGFR signaling. (*C*) Stage-14 wild-type egg chamber stained with rhodamine–phalloidin (F-actin) and DAPI (DNA) shows complete elimination of NC nuclei. (*D–G*) Late-stage egg chambers of the indicated genotypes stained as in *C*. Note the strong dumpless phenotypes caused by cic^7 (*D*) and cic^8 (*G*), but not cic^5 (*E*) alleles. *F* shows a stage-14 cic^7 egg chamber rescued by the *cic-L* transgene. (*H*) Mutant Cic^8 protein expression in a stage-10 egg chamber stained with anti-HA antibody. (*I*) Late-stage cic^{Q474X} GLC egg chamber shows almost complete elimination of NCs after dumping. (*J*) Transgenic expression of Cic-$L^{Nter\text{-}HA}$ protein in a stage-10 egg chamber stained with anti-HA antibody. (*K*) Stage-14 cic^8 egg chamber rescued by the *cic-*$L^{Nter\text{-}HA}$ transgene shows significant elimination of NCs (compare with *G*). (*L*) Bar chart showing percentages of phenotypic classes for the indicated genotypes. A diagram illustrating complete (wild-type [WT]), partially affected (D1), or severely compromised (D2) dumping is shown above.

by analysis of *twist* (*twi*) gene expression in ventral regions of the embryo (*SI Appendix*, Fig. S2 *B–D*). This suggested that neither isoform is individually essential for DV patterning. In contrast, simultaneous inactivation of both isoforms using a double frameshift allele (cic^{7B}) (*SI Appendix*, *Supplementary Materials and Methods*) resulted in severe dorsalization with loss of *twi* expression (*SI Appendix*, Fig. S2*E*). These results show that Cic-L and Cic-S act redundantly in FCs during DV pattern specification.

Nevertheless, we were intrigued that, contrary to Cic-S (14, 33), Cic-L remains mostly nuclear in dorsal–anterior FCs where EGFR signaling down-regulates Cic activity (Fig. 2*B* and *SI Appendix*, Fig. S3 *A* and *A′*). While exploring the basis for this difference, we found that constitutive activation of RTK signaling via Ras^{V12} overexpression enhanced the accumulation of Cic-L in the cytoplasm (*SI Appendix*, Fig. S3*B*). This suggested that both isoforms share qualitatively similar responses to RTK signaling, although Cic-L requires higher input levels than Cic-S for localizing to the cytoplasm (*SI Appendix*, Fig. S3*C*). Supporting this interpretation, we have identified a conserved nuclear localization motif in the N-terminal region of Cic-L required for its nuclear tethering in dorsal–anterior FCs (*SI Appendix*, Fig. S3 *D* and *E*, compare with Fig. S3 *A* and *A′*).

We therefore hypothesized that, despite its preferential nuclear localization, Cic-L is functionally inactivated by EGFR signaling in dorsal–anterior FCs (*SI Appendix*, Fig. S3 *A* and *F*). Consistent with this idea, we found that clonal overexpression of Cic-L in those cells does not repress Mirr expression (*SI Appendix*, Fig. S3*G*), whereas expression of a Cic-L mutant lacking the C2 MAPK docking site, which should therefore escape EGFR-dependent down-regulation (14), efficiently does so (*SI Appendix*, Fig. S3 *F* and *H* and see *Discussion*).

Cic-L Plays Unique Essential Roles in NCs. Our expression analyses also revealed that Cic-L and Cic-S are coexpressed in NC nuclei, but with different temporal profiles: Whereas Cic-S is present from stages 3 to 10, Cic-L is only detectable from stage 8 onwards (Fig. 2 *B* and *B′*; see also below). These results raised the possibility that Cic-L and Cic-S could have different functions or regulation in NCs.

To test this idea, we first generated mosaic females carrying cic^7 germline clones (GLCs) (*SI Appendix*, *Supplementary Materials and Methods*). These females were fully sterile and laid very few collapsed eggs unable to develop. Upon dissection, their ovaries showed a dramatic "dumpless" phenotype in which NCs had failed to transfer their cytoplasm to the oocyte (Fig. 2 *C*, *D*, and *L*).

In contrast, the *cic-S*–specific allele cic^{5}, though fully sterile in homozygosis due to the requirement of Cic-S in the blastoderm embryo (1, 45, 46), did not cause any dumpless phenotypes (Fig. 2 *E* and *L*), showing that Cic-S is dispensable for NC dumping. Thus, Cic-L plays a unique role in the transfer of NC cytoplasmic components into the oocyte.

We then tested the extent to which the Cic-L N terminus contributes to the above unique function. To this end, we generated two deletion alleles that remove either most of the Cic-L N-terminal region (cic^{8}) or the N1 and Tudor-like domains simultaneously (cic^{9}) (Fig. 2*A*). We found that both mutant alleles produced semilethal females that were fully sterile and displayed qualitatively similar phenotypes to those observed in cic^{7} GLCs (Fig. 2 *D*, *G*, and *L*). Moreover, the mutant Cic^{8} protein, which carries HA epitopes in place of the Cic-L N terminus (Fig. 2*A*), displayed the same accumulation in NCs as the normal $Cic\text{-}L^{HA}$ protein (compare Fig. 2 *B* and *H*), indicating that the cic^{8} phenotype directly results from loss of the Cic-L N terminus and not from indirect effects on protein stability or localization. These results show that the Cic-L N-terminal module is critical for NC dumping.

We verified that these phenotypes result from selective inactivation of Cic-L using a *cic-L* transgene that rescued the lethal and oogenesis phenotypes caused by the cic^{7} mutation (Fig. 2 *F* and *L* and *SI Appendix, Supplementary Materials and Methods*). Consistent with these results, we found that cic^{7} GLC egg chambers display normal accumulation of Cic-S, suggesting that this isoform remains present and functional in this background and does not contribute to the observed phenotypes (*SI Appendix*, Fig. S4). Moreover, since we noted that these phenotypes resemble those uncovered by *bullwinkle* (*bwk*) mutations that map near or within the *cic* locus (47, 48), we verified that the original *bwk* mutation indeed represents a *cic-L* allele (*SI Appendix*, Fig. S5). All these results show that Cic-L has unique functions in oogenesis that require its N-terminal region.

The Cic-L N Terminus Is a Functionally Autonomous, Chromatin-Associated Module. Inspired by the structure of Proto-Cic variants (Fig. 1*A*), we then considered the possibility that a truncated version of Cic-L lacking the Cic core region might still be functional in *Drosophila*. To explore this idea, we first examined the cic^{Q474X} allele (*SI Appendix, Supplementary Materials and Methods*), a lethal mutation that introduces a premature stop codon upstream of the HMG-box and abolishes all known functions of Cic (Fig. 2*A*). Remarkably, we found that GLCs homozygous for cic^{Q474X} showed much weaker defects in oogenesis than those observed with cic^{7}, cic^{8}, or cic^{9} alleles: Dumping was clearly less affected and females laid relatively normal eggs (Fig. 2 *I* and *L*). In line with these results, the cic^{4} allele, a semilethal deletion of four conserved residues in the C1 domain that severely impairs DNA binding (Fig. 2*A*), showed no effects on dumping (Fig. 2*L*). These results suggested that the HMG-box and C1 domains, which are generally critical for Cic function, are instead largely dispensable for dumping. Confirming this idea, a genomic construct expressing the Cic-L N-terminal fragment alone ($Cic\text{-}L^{Nter}$) (Fig. 2*A*) rescued the cic^{8} dumpless phenotype (Fig. 2 *J*–*L*) and even partially restored female fertility in cic^{9} females carrying deletions of the N1 and Tudor-like domains (to a hatching rate of 22%; $n = 300$). Together, these results indicate that Cic-L–specific activity in oogenesis is mediated primarily by its unique N-terminal region.

To further explore the function of Cic-L and its isolated N-terminal fragment, and compare them with Cic-S, we examined their nuclear distributions and potential associations with chromatin in vivo. To visualize chromatin in NCs, we depleted them of Condensin II, thereby preventing the transition from polytene to dispersed polyploid chromosome organization that normally begins at stage 5 (49). In this background, endogenous Cic-L is localized at numerous sites on polytene chromosomes at stage 10 (Fig. 3*A*); these sites appear weakly stained with DAPI, indicating that Cic-L preferentially associates with decondensed chromatin domains (Fig. 3, A^{III} and A^{IV}). In contrast, Cic-S exhibits a more dispersed, looser association with polytene chromatin in those cells (Fig. 3, A^{V} and A^{VI}), suggesting that the Cic-L N terminus confers robust binding to chromatin. Indeed, removal of the Cic-L N terminus (Cic^{8} mutant, Fig. 2*A*) caused substantial disengagement from chromatin (Fig. 3*B*), whereas $Cic\text{-}L^{Nter}$ was still clearly bound to multiple chromatin sites with low DAPI signal (Fig. 3*C*). These results indicate that the Cic-L N terminus has an intrinsic chromatin-binding activity that may be critical for Cic-L regulatory function in NCs.

A related, relevant question to ask is whether Cic-L and its N-terminal region are regulated by RTK signaling in NCs. For example, the late expression pattern of Cic-L in these cells might reflect a posttranscriptional switch from high to low RTK activity allowing Cic-L accumulation from stage 8. Arguing against this idea, however, is the finding that Cic-S, which is clearly sensitive to RTK-mediated control in other contexts, does not show the same pattern of expression and is already

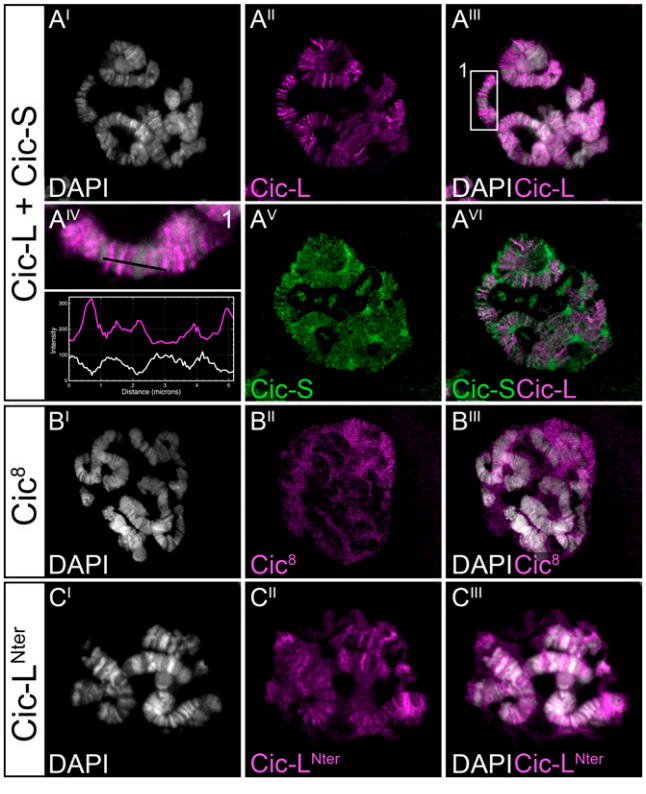

Fig. 3. Cic-L is tightly localized to NC chromatin. (*A*) Subnuclear localization of $Cic\text{-}L^{HA}$ and $Cic\text{-}S^{Venus}$ in a stage-10 NC nucleus made polytenic by depletion of the Condensin II subunit Cap-H2. Cic-L and Cic-S proteins were detected by anti-HA (magenta, A^{II}, A^{III}, and A^{VI}) and anti-GFP (green, A^{V} and A^{VI}) immunostaining, respectively. Chromosomes are stained with DAPI (white, A^{I}). Note that Cic-L is more tightly bound to chromatin than Cic-S (compare A^{II} with A^{V}). A^{IV} shows intensity profiles of Cic-L (magenta) and DAPI (white) signals along a chromosomal segment (black line) corresponding to the boxed area in A^{III}. Cic-L is concentrated in DAPI interbands. (*B* and *C*) Subnuclear distributions of Cic^{8} (*B*) and $Cic\text{-}L^{Nter}$ (*C*) proteins (Fig. 2*A*) assayed as in *A*. Only $Cic\text{-}L^{Nter}$ retains clear association to chromosomes.

detectable at earlier stages (Fig. 2*B′*). Also, the *cic-L*^{Nter} transgene, which lacks the C2 MAPK docking site, recapituales the endogenous expression of Cic-L leading to high levels of protein at stage 10 (Fig. 2*J*). Additionally, we did not find conserved potential MAPK docking sites within Cic-L^{Nter}, and below we provide evidence that its function is unaffected by high levels of constitutive Ras activity. These observations together suggest that Cic-L function in NCs is likely independent of RTK regulation.

NCs Exit the Endocycle before Dumping. To characterize the *cic-L* dumpless phenotype, we first analyzed a major cytoskeletal reorganization that takes place in NCs just prior to dumping (stage 10B). This is the formation of an actin cable array that extends from each NC cortex toward the nuclei and holds them in place as the cytoplasms flow into the oocyte (*SI Appendix*, Fig. S6*A*). These actin bundles were severely reduced or absent in *cic*^{7} GLC egg chambers (*SI Appendix*, Fig. S6 *B–D*), indicating that Cic-L is necessary for their initial assembly.

These results, together with the fact that Cic-L is already expressed ∼16 h before dumping, led us to consider the possibility that Cic-L might act at a predumping step to regulate the late stages of NC growth, perhaps as a prerequisite for dumping. How NCs transit from their growth phase to dumping is not known, but dumping is necessary for the elimination of NCs and is associated with other events that are characteristic of both apoptosis and senescence (e.g., nuclear membrane permeabilization), processes generally preceded by cell cycle arrest (50–53).

Initially, we examined the relationship between endoreplication and dumping by analyzing the temporal distributions of two key endoreplication factors, namely CycE and Double Parked (Dup)/Cdt1, in relation to actin bundle formation. During NC endocycles, CycE levels oscillate asynchronously in different NC nuclei, acting at high levels to promote CycE:Cdk2 kinase activity and entry into S phase before disappearing by the end of DNA replication (25, 26, 36). These pulses are critical for periodic control of endoreplication, and thus, forced CycE expression has been shown to block endocycle progression in other systems (25, 26, 54–58). On the other hand, Dup/Cdt1, which regulates replication licensing, accumulates during G phase (when the activity of CycE:Cdk2 kinase complexes is low) and is degraded once cells enter the S phase (59, 60) (Fig. 4*A*). We first confirmed that both CycE and Dup/Cdt1 exhibit asynchronous oscillations during NC growth from stages 2 through 9 (Fig. 4 *B* and *C*). However, clearly different patterns emerge from stage 10 onwards: Whereas Dup/Cdt1 still displays different levels among NC nuclei, CycE becomes stabilized in all nuclei (Fig. 4 *D*, *E*, and *G* and *Materials and Methods*). Using a temporal marker expressed in follicle cells, we confirmed that this stabilization is already visible at stage 10, before actin cable formation (*SI Appendix*, Fig. S7). These results suggest that CycE oscillations are subject to a mechanism of stabilization that likely leads to NC endoreplication exit at stage 10, just before the initiation of dumping. On the other hand, Dup/Cdt1 does not seem to immediately respond to this control since it remains present at different levels in NCs that have stopped cycling at stage 10.

Cic-L Is Necessary and Sufficient for NC Endoreplication Arrest and CycE Stabilization. We then asked whether CycE stabilization at stage 10 would be compromised in *cic-L* ovaries. We found that CycE is not synchronously stabilized in *cic*^{7} GLC egg chambers, since by stage 10B they still exhibit individual nuclei with either high or low levels of CycE (Fig. 4 *F* and *G*). These results suggest that Cic-L is required for NCs to exit endoreplication precisely at stage 10.

This requirement of Cic-L during stage 10 parallels its progressive accumulation in NC nuclei starting at stage 8, thus raising the possibility that Cic-L might function as the signal for endocycle termination. Hence, we tested whether Cic-L could be sufficient to induce NC growth arrest when expressed prematurely during oogenesis (Fig. 4*H*). To this end, we used the Gal4/UAS system directed by the *mat-tub-Gal4* driver, which is active in the germline from stage 2 to 3 onwards (61). Forcing early Cic-L expression yielded a dramatic phenotype in which NC growth became instantly arrested at stage 3, thus resulting in serial accumulation of tiny follicles (compare Fig. 4 *I* with *J*; see also Fig. 4*K*). The occasional presence of escaper NCs that grew larger correlated with lower levels of ectopic Cic-L expression (see below), thus confirming that Cic-L efficiently blocks NC growth. Staining of these follicles for CycE showed uniform accumulation in all NC nuclei, instead of the characteristic asynchronous fluctuations observed during normal endocycles (Fig. 4*K′*). In contrast, Dup/Cdt1 did not become either uniformly distributed or uniformly degraded in the arrested NCs (Fig. 4*K″*), which is in keeping with its persistent differential accumulation among normal stage-10 NCs that have already exited the endocycle (Fig. 4*D*). Therefore, Cic-L is sufficient to induce endocycle arrest and specific CycE stabilization. Moreover, premature expression of the Cic-L N-terminal region alone also blocks NC growth and stabilizes CycE (Fig. 4 *L* and *L′*), supporting the notion that this protein fragment is sufficient for Cic-L activity during oogenesis.

In addition, the ability of the Cic-L N-terminal module to arrest NC growth offered a useful assay to test whether its activity was modulated by RTK signaling (see above). We found that coexpression of oncogenic Ras^{V12} did not modify this effect of the Cic-L N terminus (*SI Appendix*, Fig. S8), supporting our view that this fragment is unaffected by RTK signaling.

Cic-L Induces Down-Regulation of Myc Independently of Its Effects on CycE. Having established a role of Cic-L in NC endoreplication control, we asked whether it might function exclusively via CycE or by eliciting other responses as well. In particular, we turned our attention to the Myc transcription factor, as it promotes endoreplication and growth in multiple *Drosophila* cells and tissues, including NCs (37, 38). First, we reexamined the distribution of Myc during oogenesis and found that it is present in NC nuclei throughout most of the endoreplication period (stages 2 through 9) (Fig. 5*A*), but decreases to background levels by stage 10 as NCs approach dumping (Fig. 5*B*). To test whether this decline depends on Cic-L, we examined Myc levels in *cic*^{7} GLC egg chambers and found a significant increase relative to control egg chambers (Fig. 5 *B–D*). Consistent with this effect, forced early expression of either Cic-L or its isolated N-terminal module leads to complete down-regulation of Myc as early as stage 3 (Fig. 5 *E–G*). Moreover, we monitored the response of a *Myc-lacZ* enhancer trap and found that its expression was negatively correlated with the levels of induced Cic-L (Fig. 5 *E*, *H*, and *I*), suggesting that Myc down-regulation results, at least in part, from transcriptional repression. Thus, Cic-L has opposite effects on CycE and Myc protein levels that probably contribute to its ability to suppress endoreplicative growth.

That Cic-L controls NC endoreplication via Myc and CycE is also consistent with the effects of Myc and CycE perturbations on NC growth and dumping. First, we confirmed that

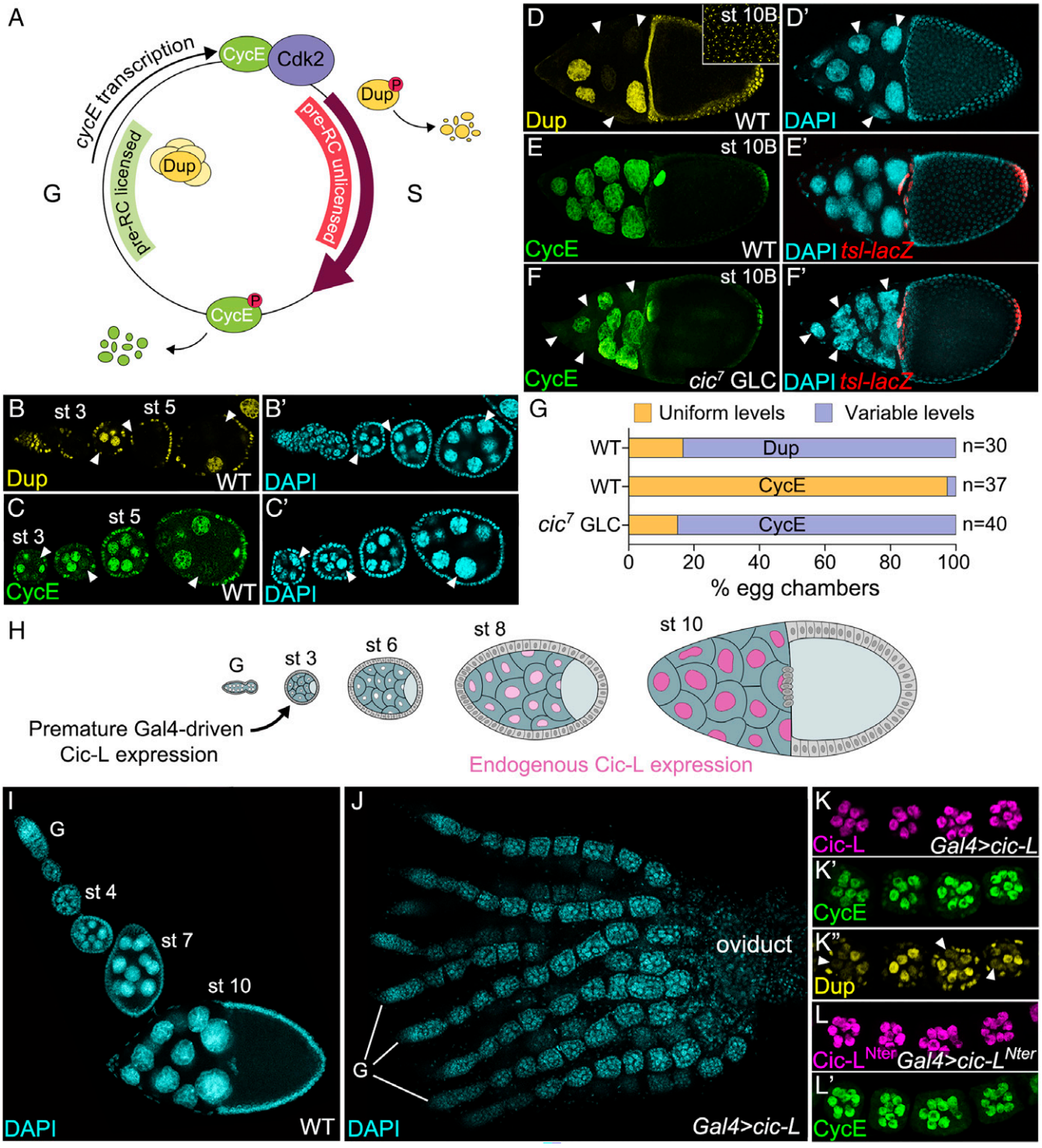

Fig. 4. Cic-L induces CycE stabilization in NCs. (*A*) Diagram of endocycle phases and periodic activities of Dup and CycE. Dup is a component of the prereplication complex (pre-RC) that licenses replication origins for DNA synthesis and is subsequently degraded as replication initiates. CycE associates with and activates Cdk2 kinase to drive progression through S phase and is down-regulated during G phase, thereby enabling assembly of the pre-RC in the next cycle. (*B*) Stage-3 to stage-6 egg chambers expressing Dup^{V5} protein and stained with anti-V5 antibody (*B*) and DAPI (*B′*). Variable levels of Dup^{V5} among NC nuclei are visible; arrowheads in this and subsequent panels point to selected nuclei devoid of protein. (*C*) Wild-type stage-3 to stage-6 egg chambers stained with anti-CycE antibody (*C*) and DAPI (*C′*). (*D*) Transgenic Dup^{V5} expression at stage 10B with DAPI staining shown in *D′*. Note the presence of Dup^{V5} in some, but not all, NC nuclei. *Inset* in *D* shows Dup^{V5} foci in follicle cell nuclei undergoing chorion amplification at stage 10B (59). (*E* and *F*) Stage-10B wild-type (*E*) and cic^{7} GLC (*F*) egg chambers stained as in *C*. Uniform accumulation of CycE is observed in wild-type but not mutant NC nuclei. *E′* and *F′* also show antibody staining against β-galactosidase expressed from the *tsl-lacZ* marker (see *SI Appendix*, Fig. S6). (*G*) Bar chart showing percentage of egg chambers with either uniform or variable levels of either Dup^{V5} or CycE proteins among NC nuclei (*Materials and Methods*). (*H*) Schematic of endogenous versus premature Gal4-driven expression of Cic-L during egg chamber development. (*I*) A wild-type ovariole stained with DAPI. (*J*) DAPI staining of an ovary expressing $Cic\text{-}L^{HA}$ under the control of the *mat-tub-Gal4* driver; all egg chambers are arrested at stage 3. G, germarium. (*K*) Egg chambers expressing full-length $Cic\text{-}L^{HA}$ protein under the control of the *mat-tub-Gal4* driver and carrying the dup^{V5} transgene and stained with anti-HA (*K*), anti-CycE (*K′*), and anti-V5 (*K″*) antibodies. CycE, but not Dup^{V5}, shows premature stabilization in all $Cic\text{-}L^{HA}$-expressing nuclei; arrowheads in *K″* indicate nuclei with low or no Dup^{V5} signal. (*L*) Egg chambers expressing $Cic\text{-}L^{Nter\text{-}HA}$ protein (Fig. 2*A*) under the control of the *mat-tub-Gal4* driver, stained with anti-HA (*L*) and anti-CycE (*L′*) antibodies. $Cic\text{-}L^{Nter\text{-}HA}$ causes stabilization of CycE as seen with full-length $Cic\text{-}L^{HA}$.

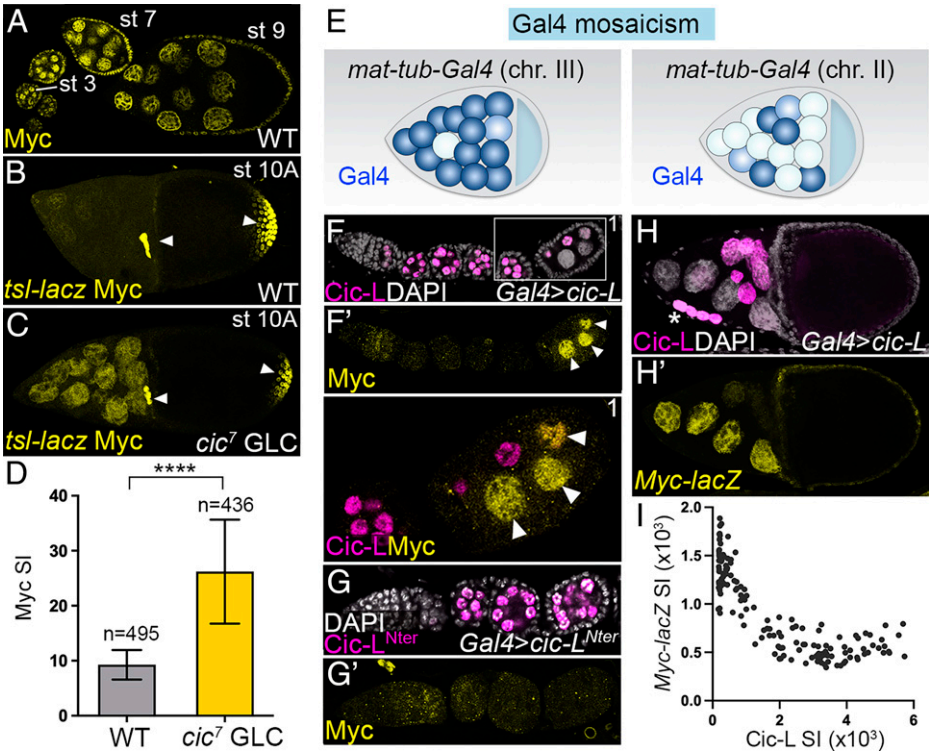

Fig. 5. Cic-L decreases Myc expression. (*A* and *B*) Distribution of Myc protein during the growth and predumping phases of NCs (stages 1 through 10A). Note that Myc levels decline until they are barely detectable by stage 10A. The egg chamber in *B* is also stained for β-galactosidase expressed from the *tsl-lacZ* marker (arrowheads, *SI Appendix*, Fig. S6). (*C*) Stage 10A cic^7 GLC egg chamber stained as in *B* showing increased accumulation of Myc in NC nuclei. (*D*) Mean signal intensity (SI) for Myc in individual NC nuclei from stage-10 wild-type and cic^7 GLC egg chambers. Statistically significant differences were determined using Student's *t* test with Welch's correction (****$P \leq 0.0001$); error bars represent the SD. (*E*) Diagram illustrating different levels of NC mosaicism due to variable Gal4 expression from two *mat-tub-Gal4* drivers, *matα4-Gal-VP16*^{V2H} and *matα4-Gal-VP16*^{V37}, inserted on chromosomes II and III, respectively (*SI Appendix, Supplementary Materials and Methods*); the chromosome II insertion shows more variable activation than the driver on chromosome III. (*F*) Egg chambers expressing full-length Cic-L^{HA} protein under the control of the third chromosome *mat-tub-Gal4* driver, and stained with anti-HA (*F*) and anti-Myc (*F'*) antibodies and DAPI (*F*). An enlarged view of merged Cic-L and Myc signals from the boxed area in *F* is shown below. Egg chambers are arrested at stage 3 and generally lack Myc protein (compare with egg chambers of the same stage in *A*). Note, however, that a few individual nuclei that have failed to express Cic-L do exhibit detectable Myc protein and are of larger size than their neighbors (arrowheads). (*G*) Egg chambers expressing Cic-L$^{Nter\text{-}HA}$ assayed as in *F*. (*H*) Egg chamber expressing full-length Cic-L^{HA} protein under the control of the chromosome II *mat-tub-Gal4* driver and carrying a *Myc-lacZ* reporter. Signals were detected as in *F* but using an anti–β-galactosidase antibody instead of anti-Myc antibody. Cic-L^{HA}-expressing nuclei show weak or no *Myc-lacZ* expression. Note the presence of four tiny NCs (asterisk in *H*) probably resulting from robust early activation of the driver. Note also that the *Myc-lacZ* reporter exhibits perdurant β-galactosidase staining in stage 10. (*I*) Scatterplot representing SI values for Cic-L and *Myc-lacZ* in individual NC nuclei analyzed as in *H*. Note the strong inverse correlation between both variables (Spearman's correlation coefficient = −0.82; $P \leq 0.0001$).

depletion of Myc as well as overexpression of CycE at early stages of oogenesis result in strong suppression of NC growth, as observed upon overexpression of Cic-L (compare Fig. 4*J* with *SI Appendix*, Fig. S9 *A* and *B*). On the other hand, consistent with the phenotype of *cic-L* mutants, overexpression of Myc from stage 3 onwards caused significant dumping defects in 72% of egg chambers ($n = 102$) (*SI Appendix*, Fig. S9*C*). Although we cannot formally rule out that this phenotype results from cumulative defects in NC function starting at stage 3, it suggests that excessive Myc activity perturbs the timely initiation of NC dumping. Consistent with this idea, Myc overexpression also causes incomplete stabilization of CycE in approximately half of stage-10 egg chambers (54%; $n = 35$) (*SI Appendix*, Fig. S9*D*), a phenotype again reminiscent of that seen in *cic-L* mutants. We note that these effects on dumping and CycE dynamics are clearly less penetrant that those seen in *cic-L* mutants, implying that Cic-L controls both processes by more than just affecting Myc. Indeed, Myc depletion in NCs does not by itself stabilize CycE (*SI Appendix*, Fig. S9*E*) and, conversely, CycE overexpression does not significantly decrease Myc levels (*SI Appendix*, Fig. S9*F*). Thus, taken together, our findings support a model in which Cic-L accumulation during midoogenesis signals endocycle exit and subsequent dumping via at least partly independent effects on Myc and CycE.

Discussion

Studies in *Drosophila* and mammals have elucidated a unifying model of Cic function as a default repressor of genes induced by RTK signaling. However, this model has been overlooking the fact that Cic exists in two conserved isoforms with alternative domains. How does each isoform contribute to Cic function in development and disease? Do they have different functions or regulation? Here we have shown that Cic-L, the less studied isoform, fulfills two very different functions in adjacent groups of cells in the *Drosophila* ovary: 1) it acts redundantly with Cic-S downstream of EGFR signaling in FCs, and 2) it functions individually as an essential regulator of endocycle exit in NCs Fig. 6. As discussed below, the deep evolutionary conservation of Cic-L proteins strongly suggests that mammalian Cic-L likely operates in a similar dual fashion.

Concerning the first function, we have demonstrated that Cic-L and Cic-S act as redundant repressors inhibited by EGFR signaling during embryonic DV polarity. These findings clarify previously observed complex relationships among *cic* alleles, including *bwk* alleles that we demonstrate are *cic-L* alleles (33, 47, 48). In addition, the combined activities of Cic-L and Cic-S suggest a similar scenario in mammals, where both isoforms overlap across multiple tissues and organs (5, 20).

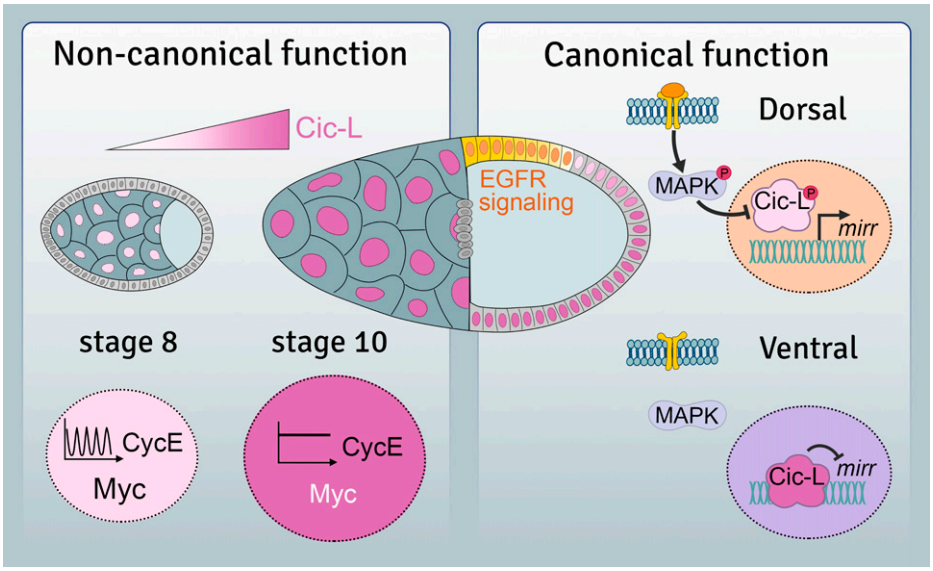

Fig. 6. Summary of canonical and noncanonical functions of Cic-L during oogenesis. During early oogenesis (stages 1 through 8), ovarian follicles grow through endoreplication of NCs, a process driven by oscillations in CycE/Cdk2 activity and the growth-promoting effects of Myc. At midoogenesis (stages 8 through 10), Cic-L begins to accumulate in NCs, where it induces endocycle exit through both stabilization of CycE and down-regulation of Myc (*Left*). This function—which, unexpectedly, does not critically depend on the canonical DNA-binding activity of Cic—is in addition essential for NC dumping from stage 11. In parallel to this germline requirment, Cic-L functions in somatic follicle cells by regulating canonical RTK-dependent responses redundantly with Cic-S (*Right*).

Related to these redundant functions, our results also indicate that Cic-S and Cic-L can be similarly down-regulated by RTK signaling irrespective of whether or not their nuclear localization is affected by the signal (*SI Appendix*, Fig. S3). These findings are consistent with prior studies showing that RTK signaling can rapidly inhibit Cic-S association with DNA before its nuclear accumulation is affected (62, 63).

Unlike all previously characterized Cic functions as a sequence-specific transcriptional repressor, the second Cic-L function studied here represents a fundamentally different type of control. This function does not critically depend on the prototypic Cic core domains, including the HMG-box and C1 DNA-binding domains and the C2 MAPK docking site. Instead, the Cic-L N terminus is largely sufficient for Cic-L function during NC development (Figs. 2 and 4). This fragment promotes strong binding of Cic-L to NC chromatin, whereas Cic-S, which is also present in NCs, shows a more diffuse distribution throughout the nucleoplasm. Therefore, Cic-L may promote changes in chromatin organization or metabolism that are essential for NC endocycle exit. This seems plausible in light of increasing evidence that chromatin transitions play critical roles in triggering or maintaining cell proliferation arrest (64, 65).

The noncanonical Cic-L function also uncovers a previously unidentified control in NCs that appears essential for their transit from endoreplicative growth to dumping. Specifically, our data support a model in which Cic-L controls NC endocycle exit by promoting both stabilization of CycE and down-regulation of Myc and suggest that these events are in turn important for dumping. The effect on CycE, in particular, is different from previously described mechanisms of cell cycle arrest associated with CycE down-regulation (35, 66). Down-regulation of CycE has also been proposed to account for endocycle exit in two different developmental systems (67, 68). Perhaps the steady accumulation of CycE in NCs during their growth-to-dumping transition has a function beyond terminating CycE oscillations.

Contrarily, Cic-L does not induce endocycle exit in FCs (*SI Appendix*, Fig. S3 *G* and *H*), which probably allows it to function in DV patterning (e.g., during stage 9) without interfering with endocycle progression. Previous studies have shown that FCs exit the endocycle during stage 10 through a combination of signals and regulators that include the Tramtrack (Ttk) transcription factor and the *miR-318* microRNA (67, 69). Neither of these regulators is expressed in late endocycling NCs (see also ref. 70), indicating that these two cell types rely on different mechanisms to terminate their endocycles. This is not entirely surprising, given that NCs and FCs follow different cellular programs after endocylce exit: Whereas NCs go into dumping and die, FCs switch to amplification of chorion loci, a process that still requires many of the components involved in whole-genome endoreplication (71, 72). Nevertheless, both exit processes are associated with down-regulation of Myc (ref. 67, and this work) and could share additional regulatory events, such as those controlling cell cycle exit of diploid cells (73–75).

Finally, our findings suggest that the noncanonical function of Cic-L has been broadly conserved during evolution. The structure of Proto-Cic variants apparently predates the archetypal configuration of Cic proteins, suggesting that those variants had a preexisting function before they combined with the HMG-box. This, and the autonomous function of the Cic-L N terminus in flies, strongly suggest that mammalian Cic-L proteins also exert isoform-specific functions through their N-terminal region. A reasonable hypothesis is that this region could play a role in endocycle control or in a pathway modulating CycE or Myc function. Such a role could represent an unknown requirement or underlie some of the known Cic-associated phenotypes that have been described in mice and humans. Thus, although it is clear that these phenotypes are often related to the activity of Cic as a repressor that recognizes TGAATGAA sites (3, 5, 10, 11), they could also involve alternative mechanisms mediated by the Cic-L N terminus. For example, impaired Cic activity in the brain derepresses *Pea3* genes as expected under the canonical model, but it also leads to down-regulation of many other genes, including some involved in neurobehavioral functions (9). This leaves open the possibility that some aspects of the associated neurological phenotypes could be due to an atypical Cic function akin to that of *Drosophila* Cic-L. Moreover, the same study identified

human mutations that create premature stop codons affecting mRNA stability and thus, potentially, the entire Cic protein complement, including the Cic-L N terminus. All these observations make it reasonable to assume that the Cic-L N terminus plays specific roles in human biology that might be disrupted in a subset of Cic-related disorders.

Materials and Methods

***Drosophila* Genetics.** The reference sequences used for Cic-S and Cic-L correspond to Cic isoforms A (National Center for Biotechnology Information [NCBI] reference sequence NP_524992.1) and D (NCBI reference sequence NP_001247203.1) in FlyBase. The *cic-L*^{HA}, *cic*^{7}, *cic*^{7B}, *cic*^{8}, *cic*^{9}, and *cic*^{10} alleles were generated via CRISPR-Cas9. Nurse cell polytene chromosomes were obtained by crossing the *matα4-Gal-VP16*^{V37} driver with the *Cap-H2*^{GL00635} RNAi line. See *SI Appendix, Supplementary Materials and Methods* for more details on alleles, transgenes, and genetic procedures used in this study.

Immunostaining and Histochemistry. Standard antibody staining and in situ hybridization techniques were used. Nurse cell polytene chromosomes were imaged using an Andor Dragonfly 505 confocal microscope. See *SI Appendix, Supplementary Materials and Methods* for further details.

Fluorescence Signal Quantification. All quantitative image analyses were performed on Fiji software. To determine the status of CycE and Dup^{V5} periodic oscillations in NC nuclei, the following scheme was implemented: First, we determined the background level for each egg chamber as the average of three mean gray values corresponding to cytoplasmic areas selected from different focal planes. We then obtained mean gray values for a representative plane of each NC nucleus and subtracted the background intensity calculated in the egg chamber. Next, the average value of the two highest nuclear signals in a given egg chamber was selected as a reference for the remaining nuclear intensities. We then considered that an egg chamber displayed asynchronous nuclear cycles in NCs when at least two nuclei had signals eight times lower than the maximum reference value. Otherwise, an egg chamber was scored as showing stabilized CycE or Dup^{V5} patterns. Myc signals in wild-type and mutant egg chambers were quantified as above and scored in parallel using the same confocal microscope settings. No background subtraction was applied in this case, as wild-type samples often showed higher cytoplasmic than nuclear signals. Cic-L^{HA} and *Myc-lacZ* (β-galactosidase) expression was measured as for Myc. All data were analyzed and represented using GraphPad Prism 5 software.

Data Availability. All study data are included in the article and/or supporting information.

ACKOWLEDGEMENTS. We thank Ainoa Olza for *Drosophila* injections; Elena Rebollo for microscopy support; Marco Milán, Ken Moberg, Ze'ev Paroush, and Stanislav Shvartsman for discussions; and Marc Furriols and the Bloomington *Drosophila* Stock Center for fly strains. We are also greatly indebted to Dolores Cortés, Sara Díez, and Núria Samper for technical assistance, and to Marco Grillo and Josep Vilardell for bioinformatic advice. This work was funded by the Spanish Government (grants BFU2014-52863-P, BFU2017-87244-P, and PID2020-119248GB-I00), the Generalitat de Catalunya (Grant 2017 SGR 475), and the NIH (Grant GM141843). L.R.-M. and C.L. were supported by predoctoral contracts from the Spanish Government.

1. G. Jiménez, A. Guichet, A. Ephrussi, J. Casanova, Relief of gene repression by torso RTK signaling: Role of *capicua* in *Drosophila* terminal and dorsoventral patterning. *Genes Dev.* **14**, 224–231 (2000).
2. A. S. K. Tseng *et al.*, Capicua regulates cell proliferation downstream of the receptor tyrosine kinase/ras signaling pathway. *Curr. Biol.* **17**, 728–733 (2007).
3. Q. Tan *et al.*, Loss of Capicua alters early T cell development and predisposes mice to T cell lymphoblastic leukemia/lymphoma. *Proc. Natl. Acad. Sci. U.S.A.* **115**, E1511–E1519 (2018).
4. L. Ajuria *et al.*, Capicua DNA-binding sites are general response elements for RTK signaling in *Drosophila*. *Development* **138**, 915–924 (2011).
5. Y. Lee *et al.*, ATXN1 protein family and CIC regulate extracellular matrix remodeling and lung alveolarization. *Dev. Cell* **21**, 746–757 (2011).
6. C. Bettegowda *et al.*, Mutations in *CIC* and *FUBP1* contribute to human oligodendroglioma. *Science* **333**, 1453–1455 (2011).
7. J. D. Fryer *et al.*, Exercise and genetic rescue of SCA1 via the transcriptional repressor Capicua. *Science* **334**, 690–693 (2011).
8. Y. Jin *et al.*, EGFR/Ras signaling controls *Drosophila* intestinal stem cell proliferation via Capicua-regulated genes. *PLoS Genet.* **11**, e1005634 (2015).
9. H. C. Lu *et al.*, Disruption of the ATXN1-CIC complex causes a spectrum of neurobehavioral phenotypes in mice and humans. *Nat. Genet.* **49**, 527–536 (2017).
10. R. A. Okimoto *et al.*, Inactivation of Capicua drives cancer metastasis. *Nat. Genet.* **49**, 87–96 (2017).
11. L. Simón-Carrasco *et al.*, Inactivation of Capicua in adult mice causes T-cell lymphoblastic lymphoma. *Genes Dev.* **31**, 1456–1468 (2017).
12. G. Jiménez, S. Y. Shvartsman, Z. Paroush, The Capicua repressor–A general sensor of RTK signaling in development and disease. *J. Cell Sci.* **125**, 1383–1391 (2012).
13. L. Simón-Carrasco, G. Jiménez, M. Barbacid, M. Drosten, The Capicua tumor suppressor: A gatekeeper of Ras signaling in development and cancer. *Cell Cycle* **17**, 702–711 (2018).
14. S. Astigarraga *et al.*, A MAPK docking site is critical for downregulation of Capicua by Torso and EGFR RTK signaling. *EMBO J.* **26**, 668–677 (2007).
15. K. Dissanayake *et al.*, ERK/p90(RSK)/14-3-3 signalling has an impact on expression of PEA3 Ets transcription factors via the transcriptional repressor *capicúa*. *Biochem. J.* **433**, 515–525 (2011).
16. Y. Ren *et al.*, CIC is a mediator of the ERK1/2-DUSP6 negative feedback loop. *iScience* **23**, 101635 (2020).
17. M. Kawamura-Saito *et al.*, Fusion between *CIC* and *DUX4* up-regulates *PEA3* family genes in Ewing-like sarcomas with t(4;19)(q35;q13) translocation. *Hum. Mol. Genet.* **15**, 2125–2137 (2006).
18. M. Forés *et al.*, A new mode of DNA binding distinguishes Capicua from other HMG-box factors and explains its mutation patterns in cancer. *PLoS Genet.* **13**, e1006622 (2017).
19. A. S. Futran, S. Kyin, S. Y. Shvartsman, A. J. Link, Mapping the binding interface of ERK and transcriptional repressor Capicua using photocrosslinking. *Proc. Natl. Acad. Sci. U.S.A.* **112**, 8590–8595 (2015).
20. Y. C. Lam *et al.*, ATAXIN-1 interacts with the repressor Capicua in its native complex to cause SCA1 neuropathology. *Cell* **127**, 1335–1347 (2006).
21. A. C. Spradling, "Developmental genetics of oogenesis" in *The Development of Drosophila Melanogaster* (1993), pp. 1–70. Cold Spring Harbor Laboratory Press, Cold Spring Harbor, NY.
22. O. Alexandrova, M. Schade, A. Böttger, C. N. David, Oogenesis in *Hydra*: Nurse cells transfer cytoplasm directly to the growing oocyte. *Dev. Biol.* **281**, 91–101 (2005).
23. R. Bastock, D. St Johnston, *Drosophila* oogenesis. *Curr. Biol.* **18**, R1082–R1087 (2008).
24. L. Lei, A. C. Spradling, Mouse oocytes differentiate through organelle enrichment from sister cyst germ cells. *Science* **352**, 95–99 (2016).
25. H. O. Lee, J. M. Davidson, R. J. Duronio, Endoreplication: Polyploidy with purpose. *Genes Dev.* **23**, 2461–2477 (2009).
26. B. A. Edgar, N. Zielke, C. Gutierrez, Endocycles: A recurrent evolutionary innovation for post-mitotic cell growth. *Nat. Rev. Mol. Cell Biol.* **15**, 197–210 (2014).
27. T. L. Orr-Weaver, When bigger is better: The role of polyploidy in organogenesis. *Trends Genet.* **31**, 307–315 (2015).
28. A. K. Timmons *et al.*, Phagocytosis genes nonautonomously promote developmental cell death in the *Drosophila* ovary. *Proc. Natl. Acad. Sci. U.S.A.* **113**, E1246–E1255 (2016).
29. J. Imran Alsous *et al.*, Dynamics of hydraulic and contractile wave-mediated fluid transport during *Drosophila* oogenesis. *Proc. Natl. Acad. Sci. U.S.A.* **118**, e2019749118 (2021).
30. C. A. Doherty, R. Diegmiller, M. Kapasiawala, E. R. Gavis, S. Y. Shvartsman, Coupled oscillators coordinate collective germline growth. *Dev. Cell* **56**, 860–870.e8 (2021).
31. S. Roth, J. A. Lynch, Symmetry breaking during *Drosophila* oogenesis. *Cold Spring Harb. Perspect. Biol.* **1**, a001891 (2009).
32. D. S. Stein, L. M. Stevens, Maternal control of the *Drosophila* dorsal-ventral body axis. *Wiley Interdiscip. Rev. Dev. Biol.* **3**, 301–330 (2014).
33. D. J. Goff, L. A. Nilson, D. Morisato, Establishment of dorsal-ventral polarity of the *Drosophila* egg requires capicua action in ovarian follicle cells. *Development* **128**, 4553–4562 (2001).
34. M. J. Andreu *et al.*, Mirror represses *pipe* expression in follicle cells to initiate dorsoventral axis formation in *Drosophila*. *Development* **139**, 1110–1114 (2012).
35. J. A. Knoblich *et al.*, Cyclin E controls S phase progression and its down-regulation during *Drosophila* embryogenesis is required for the arrest of cell proliferation. *Cell* **77**, 107–120 (1994).
36. M. A. Lilly, A. C. Spradling, The *Drosophila* endocycle is controlled by Cyclin E and lacks a checkpoint ensuring S-phase completion. *Genes Dev.* **10**, 2514–2526 (1996).
37. S. B. Pierce *et al.*, dMyc is required for larval growth and endoreplication in *Drosophila*. *Development* **131**, 2317–2327 (2004).
38. J. Z. Maines, L. M. Stevens, X. Tong, D. Stein, *Drosophila* dMyc is required for ovary cell growth and endoreplication. *Development* **131**, 775–786 (2004).
39. G. Faure, I. Callebaut, Identification of hidden relationships from the coupling of hydrophobic cluster analysis and domain architecture information. *Bioinformatics* **29**, 1726–1733 (2013).
40. S. L. Fernandez-Valverde, A. D. Calcino, B. M. Degnan, Deep developmental transcriptome sequencing uncovers numerous new genes and enhances gene annotation in the sponge *Amphimedon queenslandica*. *BMC Genomics* **16**, 387 (2015).
41. M. Srivastava *et al.*, The *Trichoplax* genome and the nature of placozoans. *Nature* **454**, 955–960 (2008).
42. K. Kamm, H. J. Osigus, P. F. Stadler, R. DeSalle, B. Schierwater, *Trichoplax* genomes reveal profound admixture and suggest stable wild populations without bisexual reproduction. *Sci. Rep.* **8**, 11168 (2018).
43. O. Grimm *et al.*, Torso RTK controls Capicua degradation by changing its subcellular localization. *Development* **139**, 3962–3968 (2012).
44. M. R. Atkey, J. F. B. Lachance, M. Walczak, T. Rebello, L. A. Nilson, Capicua regulates follicle cell fate in the *Drosophila* ovary through repression of *mirror*. *Development* **133**, 2115–2123 (2006).
45. A. Papagianni *et al.*, Capicua controls Toll/IL-1 signaling targets independently of RTK regulation. *Proc. Natl. Acad. Sci. U.S.A.* **115**, 1807–1812 (2018).
46. M. Forés *et al.*, Origins of context-dependent gene repression by capicua. *PLoS Genet.* **11**, e1004902 (2015).
47. K. R. Rittenhouse, C. A. Berg, Mutations in the *Drosophila* gene *bullwinkle* cause the formation of abnormal eggshell structures and bicaudal embryos. *Development* **121**, 3023–3033 (1995).
48. F. Roch, G. Jiménez, J. Casanova, EGFR signalling inhibits Capicua-dependent repression during specification of *Drosophila* wing veins. *Development* **129**, 993–1002 (2002).

49. T. A. Hartl, H. F. Smith, G. Bosco, Chromosome alignment and transvection are antagonized by condensin II. *Science* **322**, 1384–1387 (2008).
50. D. L. Berry, E. H. Baehrecke, Growth arrest and autophagy are required for salivary gland cell degradation in *Drosophila*. *Cell* **131**, 1137–1148 (2007).
51. A. Kramer *et al.*, Apoptosis leads to a degradation of vital components of active nuclear transport and a dissociation of the nuclear lamina. *Proc. Natl. Acad. Sci. U.S.A.* **105**, 11236–11241 (2008).
52. A. Ivanov *et al.*, Lysosome-mediated processing of chromatin in senescence. *J. Cell Biol.* **202**, 129–143 (2013).
53. R. Kumari, P. Jat, Mechanisms of cellular senescence: Cell cycle arrest and senescence associated secretory phenotype. *Front. Cell Dev. Biol.* **9**, 645593 (2021).
54. A. Weiss, A. Herzig, H. Jacobs, C. F. Lehner, Continuous Cyclin E expression inhibits progression through endoreduplication cycles in *Drosophila*. *Curr. Biol.* **8**, 239–242 (1998).
55. P. J. Follette, R. J. Duronio, P. H. O'Farrell, Fluctuations in cyclin E levels are required for multiple rounds of endocycle S phase in *Drosophila*. *Curr. Biol.* **8**, 235–238 (1998).
56. S. Ekholm-Reed *et al.*, Deregulation of cyclin E in human cells interferes with prereplication complex assembly. *J. Cell Biol.* **165**, 789–800 (2004).
57. V. Chandrasekaran, S. K. Beckendorf, Tec29 controls actin remodeling and endoreplication during invagination of the *Drosophila* embryonic salivary glands. *Development* **132**, 3515–3524 (2005).
58. A. Hong *et al.*, The cyclin-dependent kinase inhibitor Dacapo promotes replication licensing during *Drosophila* endocycles. *EMBO J.* **26**, 2071–2082 (2007).
59. A. J. Whittaker, I. Royzman, T. L. Orr-Weaver, *Drosophila* double parked: A conserved, essential replication protein that colocalizes with the origin recognition complex and links DNA replication with mitosis and the down-regulation of S phase transcripts. *Genes Dev.* **14**, 1765–1776 (2000).
60. M. Thomer, N. R. May, B. D. Aggarwal, G. Kwok, B. R. Calvi, *Drosophila double-parked* is sufficient to induce re-replication during development and is regulated by cyclin E/CDK2. *Development* **131**, 4807–4818 (2004).
61. A. M. Hudson, L. Cooley, Methods for studying oogenesis. *Methods* **68**, 207–217 (2014).
62. B. Lim *et al.*, Kinetics of gene derepression by ERK signaling. *Proc. Natl. Acad. Sci. U.S.A.* **110**, 10330–10335 (2013).
63. S. E. Keenan *et al.*, Rapid dynamics of signal-dependent transcriptional repression by Capicua. *Dev. Cell* **52**, 794–801.e4 (2020).
64. R. Zhang *et al.*, Formation of MacroH2A-containing senescence-associated heterochromatin foci and senescence driven by ASF1a and HIRA. *Dev. Cell* **8**, 19–30 (2005).
65. A. Blais, C. J. C. van Oevelen, R. Margueron, D. Acosta-Alvear, B. D. Dynlacht, Retinoblastoma tumor suppressor protein-dependent methylation of histone H3 lysine 27 is associated with irreversible cell cycle exit. *J. Cell Biol.* **179**, 1399–1412 (2007).
66. N. Tapon *et al.*, *salvador* Promotes both cell cycle exit and apoptosis in *Drosophila* and is mutated in human cancer cell lines. *Cell* **110**, 467–478 (2002).
67. J. Sun, L. Smith, A. Armento, W. M. Deng, Regulation of the endocycle/gene amplification switch by Notch and ecdysone signaling. *J. Cell Biol.* **182**, 885–896 (2008).
68. T. Nakano *et al.*, Targeted disruption of Pparγ1 promotes trophoblast endoreplication in the murine placenta. *bioRxiv* (2020) 10.1101/2020.05.28.120691.
69. W. Ge *et al.*, Regulation of pattern formation and gene amplification during *Drosophila* oogenesis by the miR-318 microRNA. *Genetics* **200**, 255–265 (2015).
70. R. L. French, K. A. Cosand, C. A. Berg, The *Drosophila* female sterile mutation *twin peaks* is a novel allele of *tramtrack* and reveals a requirement for Ttk69 in epithelial morphogenesis. *Dev. Biol.* **253**, 18–35 (2003).
71. B. R. Calvi, M. A. Lilly, A. C. Spradling, Cell cycle control of chorion gene amplification. *Genes Dev.* **12**, 734–744 (1998).
72. J. M. Claycomb, T. L. Orr-Weaver, Developmental gene amplification: Insights into DNA replication and gene expression. *Trends Genet.* **21**, 149–162 (2005).
73. L. A. Buttitta, A. J. Katzaroff, B. A. Edgar, A robust cell cycle control mechanism limits E2F-induced proliferation of terminally differentiated cells in vivo. *J. Cell Biol.* **189**, 981–996 (2010).
74. S. Ruijtenberg, S. van den Heuvel, G1/S Inhibitors and the SWI/SNF complex control cell-cycle exit during muscle differentiation. *Cell* **162**, 300–313 (2015).
75. Y. Ma, D. J. McKay, L. Buttitta, Changes in chromatin accessibility ensure robust cell cycle exit in terminally differentiated cells. *PLoS Biol.* **17**, e3000378 (2019).
76. J. Jumper *et al.*, Highly accurate protein structure prediction with AlphaFold. *Nature* **596**, 583–589 (2021).